Targeted Deletion of the Vesicular Nucleotide Transporter in Murine Astrocytes Impacts Central Dopamine Exocytosis

A thesis submitted by Lingyun Li

in partial fulfillment of the requirements for the degree of

Master of Science

in

Pharmacology and Drug Development

Tufts University

Graduate School of Biomedical Sciences

May 2023

Advisor: Pothos, Emmanuel N., PhD

Abstract

This project investigates the role of vesicular nucleotide transporter (VNUT) in astrocytes in modulating central dopamine exocytosis. ATP is involved in complex cellular processes, including neurotransmission and purinergic signaling. Earlier work has shown that insulin signaling is critical in regulating exocytosis of ATP in astrocytes. The current hypothesis is that impaired vesicular storage of ATP in astrocytes will lead to a reduction in dopamine release and depressive-like behavior, like mice null for the glial insulin receptor (GIRKOs). In the present study, we employed a new mouse model, tamoxifen-induced astrocyte-specific VNUTKO male mice (iA-VNUTKOs). The mice were further divided into naïve groups and chronic mild stress (CMS) groups and acute coronal brain slices of regions targeted by dopamine cell bodies such as the nucleus accumbens and dorsal striatum were exposed to the ATP analogue 2-MeS-ATP. Carbon fiber amperometry was used to quantify dopamine release in real time. In our data analysis, we considered whether iA-VNUTKO mice exhibit ameliorated dopamine exocytosis compared to VNUT-flox mice and whether iA-VNUTKO mice show a decreased dopamine response after CMS. The results of the study provide insight into the role of VNUT in regulating dopamine signaling and could potentially lead to the development of new treatments for mood disorders.

Acknowledgements

I would like to express my appreciation to current and previous lab members who assisted me in experiments: Yahia Abuhasan, Jeremy Yang, Yangyang Liu and Wenhui Li. I am also grateful to Dr. Margery Beinfeld for her assistance as my second thesis reviewer. Finally, I would like to express my deepest appreciation to my advisor, Dr. Emmanuel Pothos, for his continuous support for my project. His guidance helped me in conducting my research and thesis work.

Table of contents

List of Tables

List of Figures

List of Abbreviations

A--Avogadro constant
aCSF--Artificial solution of cerebrospinal fluid
AUC--Area under the Curve
CMS--chronic mild stress
CNS--Central Nervous System
DA--Dopamine
DS--Dorsal striatum
F--Faraday constant
GIRKO--mice null for the astrocytic IR
iA--VNUTKO-tamoxifen-induced astrocyte-specific VNUTKO mice
i.p.--intraperitoneal injection
IR--Insulin receptor
K-ATP--ATP-sensitive potassium channels
mGluR5--Metabotropic glutamate receptor 5
NAc--Nucleus Accumbens
NIRKO--Neuronal Insulin Receptor Knock-Out mice
NYIT--New York Institute of Technology
P2Rs--ATP activates purinergic receptors
SEM--standard error of the mean
VNUTs--Vesicular Nucleotide Transporters
2-MeS-ATP--2-methylthioadenosine triphosphate

Chapter 1: Introduction

1.1 Background

Astrocytes are the dominant glial cell type in the central nervous system (CNS)[1]. They exert numerous essential functions to support and maintain neurons, such as regulation of the CNS blood flow, energy and metabolism, and maintenance of ion, fluid and transmitter homeostasis[2–4].

Adenosine triphosphate (ATP) is a nucleoside triphosphate that provides energy for different processes in living cells and also serves as a neurotransmitter[5,6]. ATP hydrolysis is an important source of energy for many essential processes in organisms and cells. The main functions of ATP include intracellular and extracellular signaling, DNA and RNA synthesis, purinergic signaling, synaptic signaling, active transport, and muscle contraction[7,8] .

Previous work has showed that insulin signaling is critical in regulating exocytosis of ATP in astrocytes. The insulin receptor (IR) in astrocytes activates ATP exocytosis when bound by insulin[9]. Cytosolic ATP is transported into vesicles by the vesicular nucleotide transporter (VNUT) [10] and stored in secretory vesicles[11]. Furthermore, vesicular storage of ATP is an initiative stage of purinergic chemical transmission[12].

Dopamine release in the brain is related to multiple and complex mechanisms. ATP interacts with certain receptors which can modulate dopamine release. For example, ATP activates purinergic receptors (P2Rs) in dopaminergic neurons[13]. Also, ATP-sensitive potassium channels (K-ATPs) are expressed on cell plasma membrane in neurons, and linked to cell membrane electrical activity[14,15]. Finally, dopamine reuptake transporter and mitochondrial Mao A and B also affect dopamine release[16].

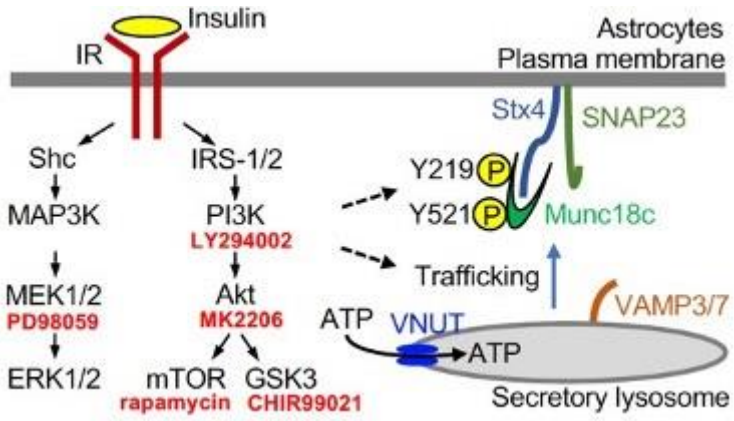

Figure 1.1 Proposed mechanism of insulin-induced exocytosis of ATP

The hypothesis of the current project is that impaired vesicular storage of ATP in astrocytes will decouple downstream IR signaling and ATP exocytosis (Figure 1.1) and will lead to dopamine release reduction in the brain as that observed in mice null for the astrocytic IR (GIRKOs)[9]. This defect may cause depressive-like behavior in VNUT deficient mice similar to GIRKOs, possibly complemented by systemic insulin and glucose dysregulation[17].

1.2 Experimental Design

To investigate the role of the VNUT in modulating the astrocytic exocytosis of ATP on dopamine signaling, we developed an animal model to inhibit ATP exocytosis by selectively deleting VNUT in astrocytes. VNUT knockout mice lack vesicular ATP storage, which leads to a decrease or elimination of ATP exocytosis in astrocytes, impacting neuronal synaptic transmission.

In this study, we employed eight groups of male mice in total, featuring two genotypes, VNUT-flox mice and tamoxifen-induced astrocyte-specific VNUTKO mice

(iA-VNUTKO), all produced in the laboratory of our collaborator, Dr. Weikang Cai, at NYIT. In order to generate iA-VNUTKO mice, the VNUT-flox mice were mated to astrocyte-specific Aldh1l1-CreERT2 mice. Both groups received tamoxifen at the age of week 6 to induce a genomic recombination[18]. VNUT-flox mice worked as control littermates in the experiment.

Both VNUT-flox and iA-VNUTKO mice were divided into naïve groups and chronic mild stress (CMS) groups. CMS mice were used to approximate an insulin receptor knockout mouse with depressive-like behavior[19] and to evaluate whether iA-VNUTKO mice are susceptible to mood disorders similar to Neuronal Insulin Receptor Knock-Out (NIRKO) mice[9] and astrocyte-specific insulin receptor knockout (GIRKO) mice[16]. Behavioral phenotypes of those three genotypes should be similar if the hypothesis linking insulin, ATP and dopamine is correct.

The four groups were further subdivided into those treated with or without 2-methylthioadenosine triphosphate **(**2-MeS-ATP) (Tocris Biosciences # 10-621-0) , an agonist for P_{2Y} receptors[20]. Thus, the eight groups studied include: flox-naïve-before 2-MeS-ATP, KO-naïve-before 2-MeS-ATP, flox-CMS-before 2-MeS-ATP, KO-CMS-before 2-MeS-ATP, flox-naïve-post 2-MeS-ATP, KO-naïve-post 2-MeS-ATP, flox-CMS-post 2-MeS-ATP, KO-CMS-post 2-MeS-ATP, respectively.

Carbon fiber amperometry was used to quantify dopamine release in the nucleus accumbens (NAc) and dorsal striatum (DS) in acute coronal brain slices *ex vivo* from those eight groups of mice. The midbrain dopamine system includes three major projections from the substantia nigra pars compacta of the striatum, and from the ventral

tegmental area to the nucleus accumbens (NAc)[21] and prefrontal cortex[22]. We will focus on DA exocytosis from the striatum and NAc in our study.

The first part of our hypothesis is that slices from iA-VNUTKO mice should exhibit ameliorated dopamine exocytosis in comparison to VNUT-flox mice. Furthermore, iA-VNUTKO mice should show blunted dopamine response after CMS. Our additional estimate is that exposure to 2-MeS-ATP will result in no increase of electrically evoked dopamine release in iA-VNUTKO brain slices, but it may present an effect in slices from VNUT-flox mice. In other words, since iA-VNUTKO mice may have a reduced ability to release ATP due to compromised ability to store ATP in vesicles, the activation of P_{2Y}-purine receptor[23] by 2-MeS-ATP may result in a weaker response or no response at all.

1.3 Statement of contributions

Figure 1.1 was reprinted with permission from E. Pothos, unpublished communication.

Chapter 2: Materials and Methods

2.1 Construction of Carbon Fiber Microelectrodes

For each electrode, a 5-um diameter single carbon fiber (Amoco Polymers Inc.) was inserted into a microfilament glass capillary. Then a Sutter Instruments P-87 flaming/brown micropipette puller was used to pull the capillary to form a sharp tip [24]. After tips were cut with a blade, the glass and carbon fiber were sealed with epoxy for 2 minutes then were placed into a 90℃ oven for 12 hours to cure. Prior to use, carbon fiber electrodes were beveled at a 45^{o} angle for 1 min and 50 seconds[25]. Carbon fiber electrodes were backfilled with a solution of 3M potassium chloride and set at a potential of 700 mV to provide an electrical circuit with an Ag/AgCl ground wire.

2.2 Experimental animals

All animal care and experimental procedures used in this study were approved by the Institutional Animal Care and Use Committees of Tufts University School of Medicine / Tufts Medical Center, as well as the New York Institute of Technology (NYIT) where the mouse lines were produced and bred. Specific iA-VNUTKO mice were achieved by daily intraperitoneal (i.p.) injections of 100 mg/kg tamoxifen solubilized in corn oil for 5 consecutive days at the age of 6 weeks. Floxed littermates without the Cre got the same regime of tamoxifen injections and were used as control groups. Exposure to chronic mild stress behavioral protocols took place in the laboratory of Dr. Cai.

2.3 Brain extraction

After a mouse was anesthetized by a mixture of 200µl xylazine and 200µl ketamine, it was decapitated by a guillotine. The top of scalp, muscles and fat on the skull were removed. Fine tweezers were used to open the midline of the back of the skull, curved spatulas were used to scoop out the brain, fine scissors were used to cut off the optic and cranial nerves. A sucrose bicarbonate solution (210mM Sucrose, 2.5mM KCl, 1.0mM $CaCl_2H_2O$, 4mM $MgCl_2 \cdot 6H_2O$, 1.25mM $NaH_2PO_4 \cdot H_2O$, 10mM Glucose, 2.6mM $NaHCO_3$ in nanopure dH_2O) was used to keep the brain before the cerebellum was removed. Ice-cold oxygenated Artificial solution of artificial cerebrospinal fluid (aCSF) (124mM NaCl, 2.0mM KCl, 1.25mM KH_2PO_4, 2mM $MgSO_4$, 25mM $NaHCO_3$, 2.0mM $CaCl_2$ and 11mM Glucose in nanopure dH2O) was used to bathe the brain slices.

2.4 Brain slicing

Holder with the vibratome blade was kept in -20℃ freezer overnight. The brain was mounted onto a Leica V1000S vibratome with agar glue on the holder. Slices were collected at a thickness of 300-microns. They were incubated in ice-cold oxygenated aCSF for at least one hour before recording.

2.5 Electrophysiology

The Axograph data acquisition software in a Mac tower computer and components of the electrophysiology rig such as two Sutter electrode micromanipulators, an Axopatch 200B amplifier, an AMPI Instruments pulse stimulator and isolator, an Olympus BX-40 microscope, a Warner Instruments temperature controller, influx and efflux lines for

aCSF and oxygen tanks to aerate solutions were all switched on. Each brain slice was then moved to the bath chamber separately, which contained oxygenated aCSF heated at physiological temperature for brain tissue (34℃). Micromanipulators lowered both the stimulating electrode (bipolar stimulation, Plastics One) and recording electrode (carbon fiber electrode) until the recording electrode's tip is placed on the brain slice. Dopamine release in the form of electrons donated by the tissue to the recording carbon fiber in an oxidation reaction (two electrons per dopamine molecule) was recorded by the amplifier, then transmitted to a digital analogue converter and finally to the computer. Each slice was stimulated both on nucleus accumbens (NAc) and dorsal striatum (DS) for three different sites, each site was stimulated and recorded from three times, each recording was performed every 5 minutes. Post-drug slices were treated with ATP analog (1% 2-MeS ATP in aCSF) for at least 40 minutes under room temperature before recording.

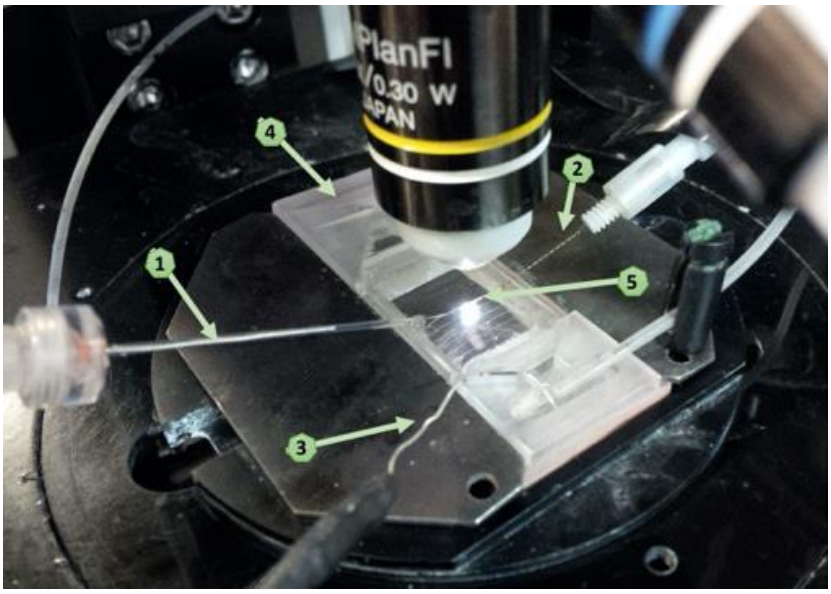

Figure 2.1 Carbon fiber amperometry setup. 1: Carbon-fiber electrode (recording electrode) 2: Stimulating electrode 3: Ground electrode (Ag/AgCl) 4: Brain slice stage 5: Acute coronal brain slice.

2.6 Data analysis and statistics

Data was analyzed through Axograph. Peak amplitude, locations, $T_{1/2}$, widths, Area Under the Curve and time constant were the parameters quantified. Average and variance calculations were done by Microsoft Excel.

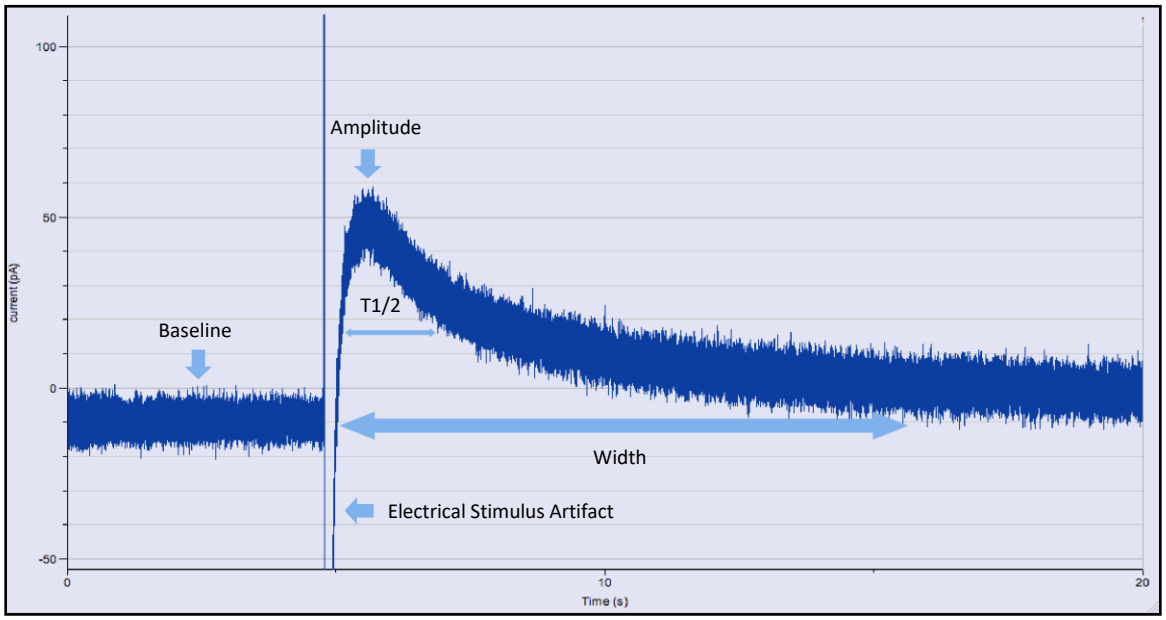

Figure 2.2 Sample of a single event of dopamine release analyzed by Axograph

The number of dopamine molecules oxidized was determined by the Faraday's equation[26]:

$$N = \frac{A \cdot \int_{t1}^{t2} Idt}{n \cdot F}$$

Where Avogadro constant (A) = 6.2 x 10^{23}, Faraday constant (F)= 96,485, n= 2 (the number of electrons transferred with each neurotransmitter molecule), t_1= the first onset time of signal rise from baseline, and t_2= the end time the signal reached baseline after t1, measured from the Area Under the Curve.

Error bars on graphs represent standard error of the mean (SEM). Data were analyzed by unpaired two-tailed t-test with Welch's correction using GraphPad Prism, as specified. $p \leq 0.05$ was considered significant. For those comparisons with nonsignificant variance, data were analyzed by unpaired two-tailed t-test, assuming both populations have the same standard deviation.

2.7 Statement of contributions

Experiments were conducted with the help of Yahia Abuhasan, Jeremy Yang, Yangyang Liu and Wenhui Li in the laboratory of Dr. Pothos. Data analysis was performed with Yahia Abuhasan, Yangyang Liu and Dr. Pothos's help. Figures 2.1 and 2.2 were reprinted with permission from E. Pothos, unpublished communication. All experiments were guided by Dr. Pothos.

Chapter 3: Results

3.1 Dopamine Molecules released in Striatum and Nucleus Accumbens

The number of dopamine molecules released were calculated both from DS and NAc slices (Table 3.1). Results showed no statistical difference among eight groups in NAc and DS slices (Figure 3.1). Specifically, none of the comparison between flox-naïve-post 2-MeS-ATP and flox-naïve-before 2-MeS-ATP, flox-CMS-post 2-MeS-ATP or KO-naïve-post 2-MeS-ATP showed any significance. The term 'naïve' refers to the control condition for CMS (chronic mild stress).

	DS		
	Mean number of molecules	SEM	sample size (animals)
flox-naïve-before 2-MeS-ATP	57672935.7	50866363.9	10
KO-naïve-before 2-MeS-ATP	94641161.0	151519376.1	10
flox-CMS-before 2-MeS-ATP	64075476.5	58780003.0	7
KO-CMS-before 2-MeS-ATP	87543349.7	139350797	8
flox-naïve-post 2-MeS-ATP	111900206.8	78456459.6	6
KO-naïve-post 2-MeS-ATP	74483830.1	57342032.4	14
flox-CMS-post 2-MeS-ATP	56083153.1	59254554.3	8
KO-CMS-post 2-MeS-ATP	50964979.7	103029543.5	8
	NAc		
	Mean number of molecules	SEM	sample size (animals)
flox- naïve -before 2-MeS-ATP	91103723.1	125715962.2	8
KO- naïve -before 2-MeS-ATP	100596028.5	118702613.9	11
flox-CMS-before 2-MeS-ATP	53755943.7	49068870.2	8
KO-CMS-before 2-MeS-ATP	267341467.5	472332003.3	4
flox-naïve-post 2-MeS-ATP	44256573.4	34168978.7	10
KO-naïve-post 2-MeS-ATP	78439433.0	79183726.0	11
flox-CMS-post 2-MeS-ATP	69294337.1	88947570.1	7
KO-CMS-post 2-MeS-ATP	40678688.1	49107307.7	5

Table 3.1 Mean±standard error of the mean (SEM) number of molecules of dopamine release from DS and NAc.

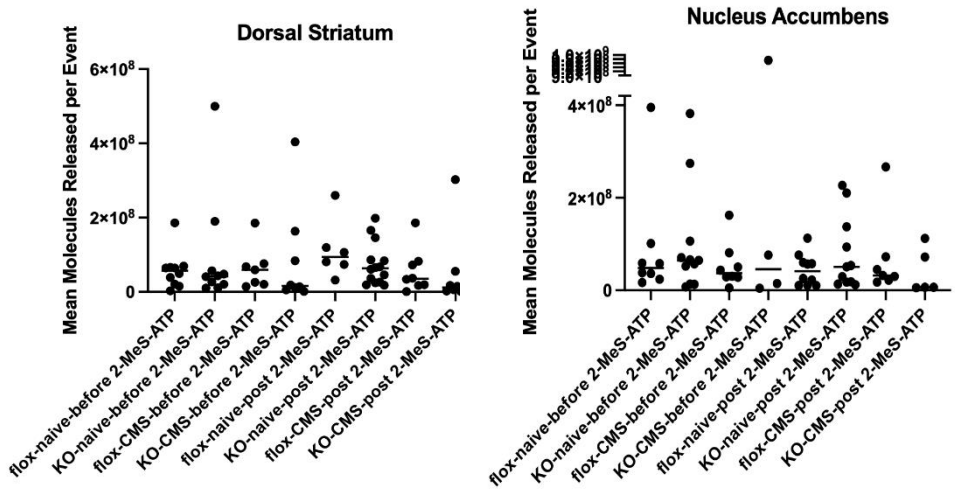

Figure 3.1 Average number of molecules of dopamine release from DS and NAc

3.2 Mean amplitude of dopamine release in Striatum and Nucleus Accumbens

Amplitude of dopamine release showed the maximum peak height from the baseline. Mean amplitude among all groups were at the range from 2000pA to 4000pA (Table 3.2). By comparing KO-naïve-post 2-MeS-ATP to flox-naïve-post 2-MeS-ATP group in NAc, the KO-naïve-post 2-MeS-ATP group showed a significantly decrease (P value=0.0385, Figure 3.2).

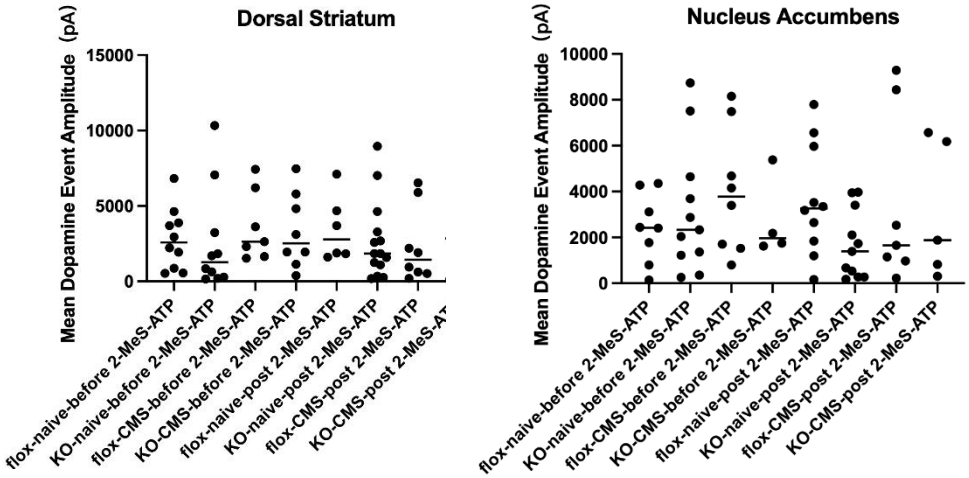

Figure 3.2 Average amplitude of dopamine release from DS and NAc

	DS		
	Mean amplitude of dopamine	SEM	sample size (animals)
flox- naïve -before 2-MeS-ATP	2806.18	2014.32	10
KO- naïve -before 2-MeS-ATP	2623.84	3422.46	10
flox-CMS-before 2-MeS-ATP	3624.07	2314.58	7
KO-CMS-before 2-MeS-ATP	3322.63	2475.06	8
flox-naïve-post 2-MeS-ATP	3467.25	2164.96	6
KO-naïve-post 2-MeS-ATP	2679.97	2587.19	14
flox-CMS-post 2-MeS-ATP	2349.96	2485.53	8
KO-CMS-post 2-MeS-ATP	3583.84	3342.24	8
	NAc		
	Mean amplitude of dopamine	SEM	sample size (animals)
flox- naïve -before 2-MeS-ATP	2411.01	1511.04	8
KO- naïve -before 2-MeS-ATP	3183.25	2790.32	11
flox-CMS-before 2-MeS-ATP	3986.83	2722.63	8
KO-CMS-before 2-MeS-ATP	2731.18	1782.63	4
flox-naïve-post 2-MeS-ATP	3621.22	2447.25	10
KO-naïve-post 2-MeS-ATP	1676.85*	1490.77	11
flox-CMS-post 2-MeS-ATP	3464.44*	3762.57	7
KO-CMS-post 2-MeS-ATP	3151.75	3001.45	5

Table 3.2 Mean±standard error of the mean (SEM) amplitude of dopamine release from DS and NAc (*$p<0.05$ between KO-naïve-post 2-MeS-ATP and flox-naïve-post 2-MeS-ATP groups).

3.3 Mean width of dopamine release in Striatum and Nucleus Accumbens

Width was calculated by the time where the peak first crosses the baseline to the first time where it crosses below the baseline. Width is indicative of neurotransmitter reuptake rate. By comparing KO-naïve-post 2-MeS-ATP to KO-CMS-post 2-MeS-ATP group in NAc, the KO-CMS-post 2-MeS-ATP group showed a significantly decrease (P value=0.0346, Figure 3.3).

	DS		
	Mean width of dopamine	SEM	sample size (animals)
flox-naïve-before 2-MeS-ATP	0.005425702	0.006041173	10
KO-naïve-before 2-MeS-ATP	0.010204244	0.010223811	10
flox-CMS-before 2-MeS-ATP	0.01651134	0.013718879	7
KO-CMS-before 2-MeS-ATP	0.008052082	0.009993138	8
flox-naïve-post 2-MeS-ATP	0.016346325	0.010421861	6
KO-naïve-post 2-MeS-ATP	0.043080297	0.137593601	14
flox-CMS-post 2-MeS-ATP	0.012501974	0.017934898	8
KO-CMS-post 2-MeS-ATP	0.006713099	0.010740564	8
	Nic		
	Mean width of dopamine	SEM	sample size (animals)
flox-naïve-before 2-MeS-ATP	0.007132545	0.008216443	8
KO-naïve-before 2-MeS-ATP	0.005283611	0.005047699	11
flox-CMS-before 2-MeS-ATP	0.005986254	0.007303992	8
KO-CMS-before 2-MeS-ATP	0.007688351	0.00807348	4
flox-naïve-post 2-MeS-ATP	0.004113932	0.007478981	10
KO-naïve-post 2-MeS-ATP	0.011199759*	0.007588781	11
flox-CMS-post 2-MeS-ATP	0.012904873	0.014803841	7
KO-CMS-post 2-MeS-ATP	0.002648275*	0.001165925	5

Table 3.3 Mean±standard error of the mean (SEM) width of dopamine release from DS and NAc (*p<0.05 between KO-naïve-post 2-MeS-ATP and KO-CMS-post 2-MeS-ATP. groups).

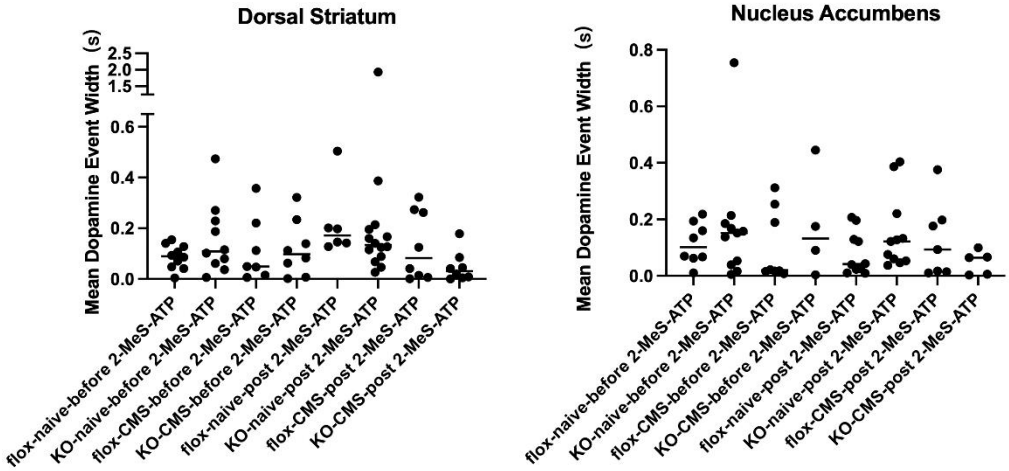

Figure 3.3 Average width of dopamine release from DS and NAc.

3.4 Mean $T_{1/2}$ of dopamine release in Striatum and Nucleus Accumbens

$T_{1/2}$ also called half width of peaks, calculated form where the width of the peak at half of its maximum amplitude. Three groups, KO-CMS-post 2-MeS-ATP (P value= 0.0039), KO-naïve-before 2-MeS-ATP (P value= 0.0456) and flox-naïve-post 2-MeS-ATP (P= 0.0445) were significantly lower than KO-naïve-post 2-MeS-ATP (Figure 3.4).

	DS		
	Mean $T_{1/2}$ of dopamine	SEM	sample size (animals)
flox-naïve-before 2-MeS-ATP	0.087216345	0.047645934	10
KO-naïve-before 2-MeS-ATP	0.156151361	0.140012659	10
flox-CMS-before 2-MeS-ATP	0.115624578	0.12932542	7
KO-CMS-before 2-MeS-ATP	0.120159032	0.110641357	8
flox-naïve-post 2-MeS-ATP	0.21997502	0.142556711	6
KO-naïve-post 2-MeS-ATP	0.270831318	0.486022296	14
flox-CMS-post 2-MeS-ATP	0.130754983	0.135341469	8
KO-CMS-post 2-MeS-ATP	0.047789157	0.059691663	8
	Nic		
	Mean $T_{1/2}$ of dopamine	SEM	sample size (animals)
flox-naïve-before 2-MeS-ATP	0.114353717	0.07308753	8
KO-naïve-before 2-MeS-ATP	0.171076156	0.206550026	11
flox-CMS-before 2-MeS-ATP	0.104244665	0.126331474	8
KO-CMS-before 2-MeS-ATP	0.178495533*	0.190868756	4
flox-naïve-post 2-MeS-ATP	0.080255483*	0.076808007	10
KO-naïve-post 2-MeS-ATP	0.1511642*, *, **	0.131676705	11
flox-CMS-post 2-MeS-ATP	0.126268637	0.134709914	7
KO-CMS-post 2-MeS-ATP	0.047759007**	0.042128109	5

Table 3.4 Mean±standard error of the mean (SEM) $T_{1/2}$ of dopamine release from DS and NAc. (*p<0.05 between KO-naïve-before 2-MeS-ATP and KO-naïve-post 2-MeS-ATP, flox-naïve-post 2-MeS-ATP and KO-naïve-post 2-MeS-ATP groups, ** p<0.005 between KO-CMS-post 2-MeS-ATP and KO-naïve-post 2-MeS-ATP groups).

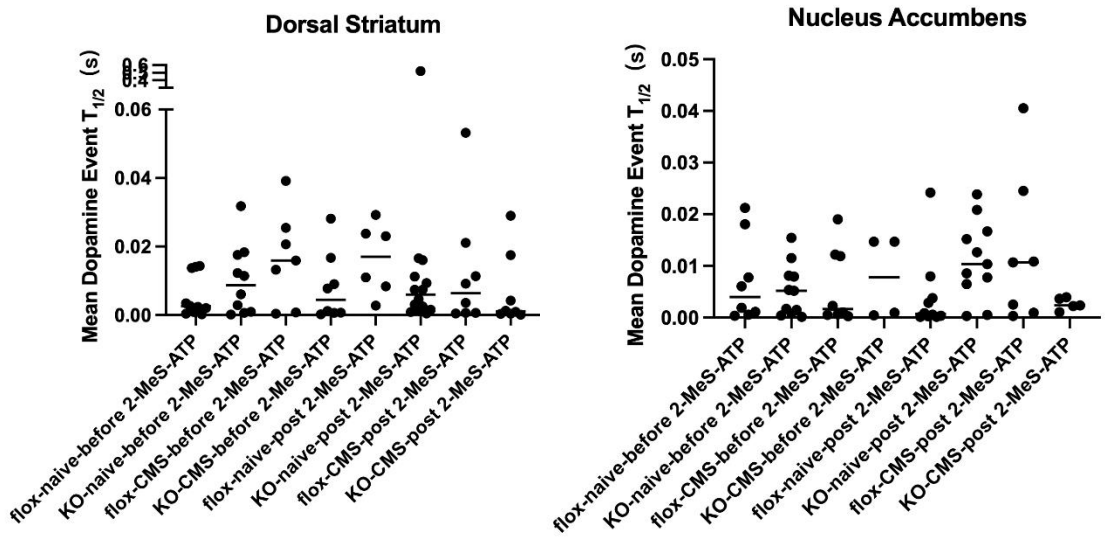

Figure 3.4 Average $T_{1/2}$ of dopamine release from DS and NAc

3.5 Mean time constant of dopamine release in Striatum and Nucleus Accumbens

The time constant also presented as time τ (tau) and were used to indicate how rapidly the exocytotic event decayed[27]. Most of mean time constant were smaller than 0.2 second (Figure 3.5).

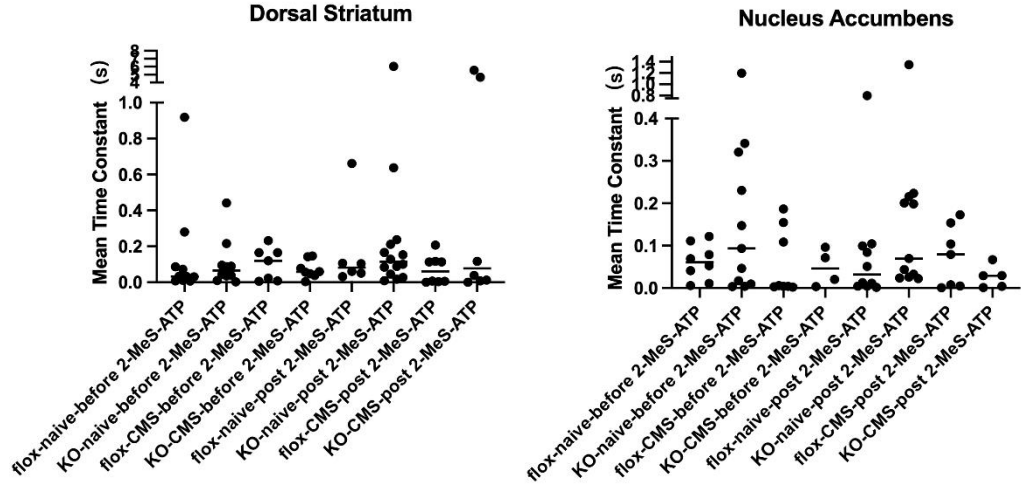

Figure 3.5 Average Time Constant of dopamine release from DS and NAc

	DS		
	Mean Time Constant of dopamine	SEM	sample size (animals)
flox-naïve-before 2-MeS-ATP	0.148113619	0.282560768	10
KO-naïve-before 2-MeS-ATP	0.106214578	0.132716602	10
flox-CMS-before 2-MeS-ATP	0.102923334	0.090882376	7
KO-CMS-before 2-MeS-ATP	0.071627365	0.049993256	8
flox-naïve-post 2-MeS-ATP	0.169063795	0.242928933	6
KO-naïve-post 2-MeS-ATP	0.567365394	1.580845827	14
flox-CMS-post 2-MeS-ATP	0.071477548	0.077614912	8
KO-CMS-post 2-MeS-ATP	1.528811644	2.306618022	8
	Nac		
	Mean Time Constant of dopamine	SEM	sample size (animals)
flox-naïve-before 2-MeS-ATP	0.061366912	0.042599453	8
KO-naïve-before 2-MeS-ATP	0.219146174	0.347864682	11
flox-CMS-before 2-MeS-ATP	0.058469079	0.078394335	8
KO-CMS-before 2-MeS-ATP	0.047876451	0.043252055	4
flox-naïve-post 2-MeS-ATP	0.117188004	0.243157848	10
KO-naïve-post 2-MeS-ATP	0.218593333	0.384585956	11
flox-CMS-post 2-MeS-ATP	0.074578294	0.072523761	7
KO-CMS-post 2-MeS-ATP	0.026147571	0.026379327	5

Table 3.5 Mean±standard error of the mean (SEM) Time Constant of dopamine release from DS and NAc

3.6 Statement of contributions

All of the figures and tables in this section were made by me.

Chapter 4: Discussion

In this study, we used carbon fiber amperometry to assess dopamine exocytosis in all tested groups of mice.

At current significance level and with the current available sample, the study shows that there is no significant statistical significance among comparisons in amplitude, dopamine molecule released, width, $T_{1/2}$ and time constant between iA-VNUTKOs and VNUT-flox (control) groups that were exposed to either chronic mild stress or an ATP analog (2-MeS-ATP) .

The KO-CMS-post 2-MeS-ATP group showed a decrease in dopamine width and width-at-half-height (t ½) signal when compared to KO-naïve-post 2-MeS-ATP group, suggesting differences in neurotransmitter uptake, perhaps consistent with a previous study showing compromised glutamate uptake after chronic stress in rats[28].

Consistent with our observations, behavioral tests on motor and depression-like behavior run by Dr. Cai's laboratory among these groups of male mice also did not uncover any significant differences. It may require an increase in statistical power to draw safe conclusions as we only examined 6-12 mice per group. Furthermore, we are now embarking on a similar study in female mice to consider whether female iA-VNUTKO mice are more susceptible to depression-like behavior and aberrations in dopamine release. Transitioning to *in vivo* assays for dopamine release may also yield different results[29]. Possibilities include single-scan dynamic molecular imaging[30], measuring dopamine levels in total brain[31,32]; and mechanically controllable break junction (MCBJ) to increase resolution and monitor single neurotransmitter molecules[33].

Furthermore, the modulation of dopamine release by ATP through potassium channels in neurons may not be the decisive mechanism affecting dopamine release in neurons. Glial synthesis of glutamate may be an alternative and we may need to consider such mechanisms in the immediate future as we try to decipher the role of brain insulin receptors in regulating dopamine exocytosis and behavior.

Glutamate is an excitatory neurotransmitter that is released by astrocytes in the brain[34,35], and plays a significant role in regulating dopamine release. More and more evidence shows that glutamatergic and dopaminergic transmission have certain reciprocal interactions[36]. Metabotropic glutamate receptor 5 (mGluR5) in astrocytes is activated by glutamate and can regulate neuronal excitability[37]. Also, co-released of dopamine and glutamate from neuronal subpopulations in the midbrain may affect dopamine neurotransmission and reward pathway [38].

In conclusion, while the modulation of dopamine release through ATP is not well established from our experiments so far, it is possible to further consider this mechanism in female mice, as well as examine alternative mechanisms such as glial synthesis of glutamate to explain the role of brain insulin receptors in regulating dopamine exocytosis and behavior.

Chapter 5: Appendix

aCSF

REAGENT	*g/500mL sol'n*	*g/L sol'n*	*g/5L sol'n*
124mM NaCl (mw 58.44)	3.623	7.247	36.235
2.0mM KCl (mw 74.55)	0.075	0.149	0.74
1.25mM KH_2PO_4 (mw 136.1)	0.085	0.170	0.850
2.0mM $MgSO_4$ (mw 120.4) or 2.0mM $MgSO_4$* $7H_2O$ (mw 246.5)	0.120 or 0.247	0.241 or 0.493	1.20 or 2.46
25mM $NaHCO_3$ (mw 84.1)	1.051	2.103	
2.0mM $CaCl_2$ (mw 111.0)	0.111	0.222	1.110
11mM Glucose (mw 180.2)	0.911	1.982	9.91

Table 5.1 reagents of aCSF solution

SUCROSE 10x STOCK SOL'N

REAGENT	*g/L*	*g/2L*	*mM (1x)*	*mM (10x)*
Sucrose (mw 342)	574.56 (80%)	1436.4	210	2100
KCl (mw 74.6)	2.61	5.22	3.5	35
$CaCl_2$ * $2H_2O$ (mw 147)	1.47	2.94	1	10
$MgCl_2$ * $6H_2O$ (mw 203)	8.12	16.24	4	40
NaH_2PO_4 * H_2O (mw 138)	1.72	3.44	1.25	12.5
Glucose (mw 180)	18	36	10	100

Table 5.2 reagents of sucrose solution

BICARBONATE 10x STOCK SOL'N

REAGENT	*g/L*
$NaHCO_3$ (mw 84)	21.84

Table 5.3 reagents of bicarbonate solution

DOPAMINE

REAGENT	*/15mL*
Dopamine hydrochloride (store in 4ºC)	17.7mg
HCLO4	387 µl

Table 5.4 reagents of dopamine

Chapter 6: Bibliography

(1) Harada, K.; Kamiya, T.; Tsuboi, T. Gliotransmitter Release from Astrocytes: Functional, Developmental and Pathological Implications in the Brain. *Frontiers in Neuroscience* **2016**, *9*.

(2) Sofroniew, M. V.; Vinters, H. V. Astrocytes: Biology and Pathology. *Acta Neuropathol* **2010**, *119* (1), 7–35. https://doi.org/10.1007/s00401-009-0619-8.

(3) Barres, B. A. The Mystery and Magic of Glia: A Perspective on Their Roles in Health and Disease. *Neuron* **2008**, *60* (3), 430–440. https://doi.org/10.1016/j.neuron.2008.10.013.

(4) Vasile, F.; Dossi, E.; Rouach, N. Human Astrocytes: Structure and Functions in the Healthy Brain. *Brain Struct Funct* **2017**, *222* (5), 2017–2029. https://doi.org/10.1007/s00429-017-1383-5.

(5) Vultaggio-Poma, V.; Sarti, A. C.; Di Virgilio, F. Extracellular ATP: A Feasible Target for Cancer Therapy. *Cells* **2020**, *9* (11), 2496. https://doi.org/10.3390/cells9112496.

(6) Miras-Portugal, M. T.; Menéndez-Méndez, A.; Gómez-Villafuertes, R.; Ortega, F.; Delicado, E. G.; Pérez-Sen, R.; Gualix, J. Physiopathological Role of the Vesicular Nucleotide Transporter (VNUT) in the Central Nervous System: Relevance of the Vesicular Nucleotide Release as a Potential Therapeutic Target. *Frontiers in Cellular Neuroscience* **2019**, *13*.

(7) Dunn, J.; Grider, M. H. Physiology, Adenosine Triphosphate. In *StatPearls*; StatPearls Publishing: Treasure Island (FL), 2022.

(8) Dahl, G. ATP Release through Pannexon Channels. *Philosophical Transactions of the Royal Society B: Biological Sciences* **2015**, *370* (1672), 20140191. https://doi.org/10.1098/rstb.2014.0191.

(9) Cai, W.; Xue, C.; Sakaguchi, M.; Konishi, M.; Shirazian, A.; Ferris, H. A.; Li, M. E.; Yu, R.; Kleinridders, A.; Pothos, E. N.; Kahn, C. R. Insulin Regulates Astrocyte Gliotransmission and Modulates Behavior. *J Clin Invest* **2018**, *128* (7), 2914–2926. https://doi.org/10.1172/JCI99366.

(10) Mielnicka, A.; Michaluk, P. Exocytosis in Astrocytes. *Biomolecules* **2021**, *11* (9), 1367. https://doi.org/10.3390/biom11091367.

(11) Sawada, K.; Echigo, N.; Juge, N.; Miyaji, T.; Otsuka, M.; Omote, H.; Yamamoto, A.; Moriyama, Y. Identification of a Vesicular Nucleotide Transporter. *Proceedings of the National Academy of Sciences* **2008**, *105* (15), 5683–5686. https://doi.org/10.1073/pnas.0800141105.

(12) Moriyama, Y.; Hiasa, M.; Sakamoto, S.; Omote, H.; Nomura, M. Vesicular Nucleotide Transporter (VNUT): Appearance of an Actress on the Stage of Purinergic Signaling. *Purinergic Signal* **2017**, *13* (3), 387–404. https://doi.org/10.1007/s11302-017-9568-1.

(13) Xiao, C.; Zhou, C.; Li, K.; Davies, D. L.; Ye, J. H. Purinergic Type 2 Receptors at GABAergic Synapses on Ventral Tegmental Area Dopamine Neurons Are Targets for Ethanol Action. *J Pharmacol Exp Ther* **2008**, *327* (1), 196–205. https://doi.org/10.1124/jpet.108.139766.

(14) Dragicevic, E.; Schiemann, J.; Liss, B. Dopamine Midbrain Neurons in Health and Parkinson's Disease: Emerging Roles of Voltage-Gated Calcium Channels and

ATP-Sensitive Potassium Channels. *Neuroscience* **2015**, *284*, 798–814. https://doi.org/10.1016/j.neuroscience.2014.10.037.
(15) Szeto, V.; Chen, N.-H.; Sun, H.-S.; Feng, Z.-P. The Role of KATP Channels in Cerebral Ischemic Stroke and Diabetes. *Acta Pharmacol Sin* **2018**, *39* (5), 683–694. https://doi.org/10.1038/aps.2018.10.
(16) Kleinridders, A.; Cai, W.; Cappellucci, L.; Ghazarian, A.; Collins, W. R.; Vienberg, S. G.; Pothos, E. N.; Kahn, C. R. Insulin Resistance in Brain Alters Dopamine Turnover and Causes Behavioral Disorders. *Proc Natl Acad Sci U S A* **2015**, *112* (11), 3463–3468. https://doi.org/10.1073/pnas.1500877112.
(17) Manaserh, I. H.; Maly, E.; Jahromi, M.; Chikkamenahalli, L.; Park, J.; Hill, J. Insulin Sensing by Astrocytes Is Critical for Normal Thermogenesis and Body Temperature Regulation. *Journal of Endocrinology* **2020**, *247* (1), 39–52. https://doi.org/10.1530/JOE-20-0052.
(18) Falke, L. L.; Broekhuizen, R.; Huitema, A.; Maarseveen, E.; Nguyen, T. Q.; Goldschmeding, R. Tamoxifen for Induction of Cre-Recombination May Confound Fibrosis Studies in Female Mice. *J Cell Commun Signal* **2017**, *11* (2), 205–211. https://doi.org/10.1007/s12079-017-0390-x.
(19) Willner, P. The Chronic Mild Stress (CMS) Model of Depression: History, Evaluation and Usage. *Neurobiol Stress* **2016**, *6*, 78–93. https://doi.org/10.1016/j.ynstr.2016.08.002.
(20) Lenz, G.; Gottfried, C.; Luo, Z.; Avruch, J.; Rodnight, R.; Nie, W.-J.; Kang, Y.; Neary, J. T. P2Y Purinoceptor Subtypes Recruit Different Mek Activators in Astrocytes. *Br J Pharmacol* **2000**, *129* (5), 927–936. https://doi.org/10.1038/sj.bjp.0703138.
(21) Nicola, S. M.; Taha, S. A.; Kim, S. W.; Fields, H. L. Nucleus Accumbens Dopamine Release Is Necessary and Sufficient to Promote the Behavioral Response to Reward-Predictive Cues. *Neuroscience* **2005**, *135* (4), 1025–1033. https://doi.org/10.1016/j.neuroscience.2005.06.088.
(22) Eisenhofer, G.; Reichmann, H. Chapter 12 - Dopaminergic Neurotransmission. In *Primer on the Autonomic Nervous System (Third Edition)*; Robertson, D., Biaggioni, I., Burnstock, G., Low, P. A., Paton, J. F. R., Eds.; Academic Press: San Diego, 2012; pp 63–65. https://doi.org/10.1016/B978-0-12-386525-0.00012-3.
(23) Keppens, S.; De Wulf, H. Characterization of the Biological Effects of 2-Methylthio-ATP on Rat Hepatocytes: Clear-Cut Differences with ATP. *Br J Pharmacol* **1991**, *104* (2), 301–304. https://doi.org/10.1111/j.1476-5381.1991.tb12426.x.
(24) Kawagoe, K. T.; Zimmerman, J. B.; Wightman, R. M. Principles of Voltammetry and Microelectrode Surface States. *Journal of Neuroscience Methods* **1993**, *48* (3), 225–240. https://doi.org/10.1016/0165-0270(93)90094-8.
(25) Bath, B. D.; Michael, D. J.; Trafton, B. J.; Joseph, J. D.; Runnels, P. L.; Wightman, R. M. Subsecond Adsorption and Desorption of Dopamine at Carbon-Fiber Microelectrodes. *Anal. Chem.* **2000**, *72* (24), 5994–6002. https://doi.org/10.1021/ac000849y.
(26) *PDF | Functional screening of established and experimental weight loss drugs in terms of their effects on central dopamine release kinetics | ID: ks65hq372 | Tufts Digital Library*. https://dl.tufts.edu/concern/pdfs/ks65hq372 (accessed 2023-02-13).

(27) Meunier, A.; Bretou, M.; Darchen, F.; Guille Collignon, M.; Lemaître, F.; Amatore, C. Amperometric Detection of Vesicular Exocytosis from BON Cells at Carbon Fiber Microelectrodes. *Electrochimica Acta* **2014**, *126*, 74–80. https://doi.org/10.1016/j.electacta.2013.07.110.
(28) Yang, C.-H.; Huang, C.-C.; Hsu, K.-S. Behavioral Stress Enhances Hippocampal CA1 Long-Term Depression through the Blockade of the Glutamate Uptake. *J. Neurosci.* **2005**, *25* (17), 4288–4293. https://doi.org/10.1523/JNEUROSCI.0406-05.2005.
(29) Roberts, J. G.; Lugo-Morales, L. Z.; Loziuk, P. L.; Sombers, L. A. Real-Time Chemical Measurements of Dopamine Release in the Brain. *Methods Mol Biol* **2013**, *964*, 275–294. https://doi.org/10.1007/978-1-62703-251-3_16.
(30) Badgaiyan, R. D. Detection of Dopamine Neurotransmission in "Real Time." *Front Neurosci* **2013**, *7*, 125. https://doi.org/10.3389/fnins.2013.00125.
(31) Oien, D. B.; Osterhaus, G. L.; Latif, S. A.; Pinkston, J. W.; Fulks, J.; Johnson, M.; Fowler, S. C.; Moskovitz, J. The MsrA Knockout Mouse Exhibits Abnormal Behavior and Brain Dopamine Levels. *Free Radic Biol Med* **2008**, *45* (2), 193–200. https://doi.org/10.1016/j.freeradbiomed.2008.04.003.
(32) Jensen, K. L.; Runegaard, A. H.; Weikop, P.; Gether, U.; Rickhag, M. Assessment of Dopaminergic Homeostasis in Mice by Use of High-Performance Liquid Chromatography Analysis and Synaptosomal Dopamine Uptake. *J Vis Exp* **2017**, No. 127, 56093. https://doi.org/10.3791/56093.
(33) Komoto, Y.; Ohshiro, T.; Yoshida, T.; Tarusawa, E.; Yagi, T.; Washio, T.; Taniguchi, M. Time-Resolved Neurotransmitter Detection in Mouse Brain Tissue Using an Artificial Intelligence-Nanogap. *Sci Rep* **2020**, *10* (1), 11244. https://doi.org/10.1038/s41598-020-68236-3.
(34) Andersen, J. V.; Markussen, K. H.; Jakobsen, E.; Schousboe, A.; Waagepetersen, H. S.; Rosenberg, P. A.; Aldana, B. I. Glutamate Metabolism and Recycling at the Excitatory Synapse in Health and Neurodegeneration. *Neuropharmacology* **2021**, *196*, 108719. https://doi.org/10.1016/j.neuropharm.2021.108719.
(35) Purves, D.; Augustine, G. J.; Fitzpatrick, D.; Katz, L. C.; LaMantia, A.-S.; McNamara, J. O.; Williams, S. M. Glutamate. *Neuroscience. 2nd edition* **2001**.
(36) Morari, M.; Marti, M.; Sbrenna, S.; Fuxe, K.; Bianchi, C.; Beani, L. Review Article Reciprocaldopamine-Glutamatemodulation of Release in the Basalganglia. *Neurochemistry International* **1998**, *33* (5), 383–397. https://doi.org/10.1016/S0197-0186(98)00052-7.
(37) Fellin, T.; D'Ascenzo, M.; Haydon, P. G. Astrocytes Control Neuronal Excitability in the Nucleus Accumbens. *TheScientificWorldJOURNAL* **1900**, *7*, 386805. https://doi.org/10.1100/tsw.2007.195.
(38) Buck, S. A.; Torregrossa, M. M.; Logan, R. W.; Freyberg, Z. Roles of Dopamine and Glutamate Co-Release in the Nucleus Accumbens in Mediating the Actions of Drugs of Abuse. *The FEBS Journal* **2021**, *288* (5), 1462–1474. https://doi.org/10.1111/febs.15496.